Journal of Catalysis 267 (2009) 50–56

Contents lists available at ScienceDirect

Journal of Catalysis

journal homepage: www.elsevier.com/locate/jcat

Liquid phase hydrogenation of α,β-unsaturated aldehydes over gold supported on iron oxides

Jennifer Lenz [a], Betiana C. Campo [b], Mariana Alvarez [c], María A. Volpe [b,*]

[a] Physical Chemistry, Saarland University, 66123 Saarbrücken, Germany
[b] Planta Piloto de Ingeniería Quimica, PLAPIQUI (UNS-CONICET) Camino La Carrindanga km 7, CC 717, (8000) Bahía Blanca, Argentina
[c] Universidad Nacional del Sur, Dpto de Química, Avda. Alem 1253, (8000) Bahía Blanca, Argentina

ARTICLE INFO

Article history:
Received 10 June 2009
Revised 23 July 2009
Accepted 23 July 2009
Available online 19 August 2009

Keywords:
Selective hydrogenation
α,β-unsaturated aldehydes
Iron oxides
Gold catalyst

ABSTRACT

Goethite, hematite, and iron oxide supported on alumina are employed as supports for gold catalysts. Several samples are prepared and are characterized by TEM, TPR, and XANES. The catalysts are tested for the liquid phase hydrogenation of crotonaldehyde and cinnamaldehyde in a Batch reactor at 100 °C and at 1 MPa of H_2 employing isopropanol as the solvent. Gold particles supported on the different iron oxides are more selective than the ones supported on an inert oxide (γ-Al_2O_3). Gold supported on hematite presents the highest selectivity toward the unsaturated alcohol. It is concluded that the promotional effect of iron on gold is neither due to the redox properties of the support nor due to the presence of charged gold particles. No dependence of selectivity to crotyl alcohol or to cinnamyl alcohol on gold particle size was observed. The origin of the improved selectivity to the unsaturated alcohol of Au/iron oxides would be related to morphological aspects of gold particles.

1. Introduction

In the last few years, gold catalysts have been employed for the hydrogenation of α,β-unsaturated compounds, and in some cases a high selectivity to the unsaturated alcohol was obtained [1–8]. Generally, the selected supports for gold catalysts are reducible oxides, such as iron oxides [3,4], TiO_2 [5], CeO_2 [6,7], and ZrO_2 [2,8–10]. It was postulated that there exists a beneficial effect of these supports on the intrinsic selectivity of gold to hydrogenate conjugated C=O bonds.

In the liquid phase hydrogenation of benzalacetone, Milone et al. reported a selectivity toward the unsaturated ketone higher than 60% (for conversion of 90%) for gold supported on iron oxides [3,4]. This is a remarkable result since no other catalyst has been found to accomplish the hydrogenation of an α,β-unsaturated ketone to the unsaturated alcohol with gaseous H_2 as the reductant. The authors concluded that the high selectivity was due to a synergic effect between gold and iron oxide, and that an electron transfer from the reduced iron oxide to the metal takes place. A similar interpretation for the high selectivity of gold for the hydrogenation of acrolein over Au/TiO_2 and Au/ZrO_2 was postulated by the group of Claus. They suggested that the enhanced hydrogenation of conjugated carbonyl groups is due to electron-rich gold particles formed by interaction with partially reduced supports [9].

A controversial aspect concerning the hydrogenation of α,β-unsaturated compounds is the effect of gold particle size on the selectivity. Zanella et al. concluded that for gold particle size within the range of 1.7–8.7 nm, the hydrogenation of crotonaldehyde over Au/TiO_2 catalysts is insensible for the structure reaction [5]. On the other hand, the group of Claus suggested that the hydrogenation of acrolein is an antipathetic structure-sensitivity reaction over Au/ZrO_2 [1,9]. However, in a later work Claus stressed the influence of the real structure gold crystals on the selectivity, giving a secondary consideration to particle size. Bailey and Hutchings studied the hydrogenation of crotonaldehyde over a series of Au/ZnO_2 catalysts, and they concluded that small gold particles (diameter <2 nm) are not selective for this reaction, but the active sites for selective hydrogenation are associated with the presence of large Au crystals [2]. Following the conclusion of Bus et al. [11], small gold clusters would be indispensable for high activity and selectivity in the hydrogenation of cinnamaldehyde over Au/γ-Al_2O_3. In a previous work, some of us concluded that the selectivity to crotyl alcohol in the hydrogenation of crotonaldehyde in liquid phase over Au/CeO_2 is notably lower for large gold particles (11 nm) than for small (4 nm) gold particles [7].

The present work focuses on the hydrogenation of two α,β-unsaturated aldehydes (crotonaldehyde and cinnamaldehyde) over gold catalysts supported on goetithe (α-FeOOH), hematite (α-Fe_2O_3), and iron species highly dispersed on γ-Al_2O_3. It could be speculated that iron species would enhance the rate of C=O

---

* Corresponding author. Fax: +54 291 4861600.
E-mail addresses: mvolpe@plapiqui.edu.ar, mvolpe@criba.edu.ar (M.A. Volpe).

0021-9517/$ - see front matter © 2009 Elsevier Inc. All rights reserved.
doi:10.1016/j.jcat.2009.07.012

hydrogenation against C=C hydrogenation. The characterization was carried out by Transmission Electron Microscopy (TEM), Temperature Programmed Reduction (TPR), and XANES spectroscopy. Probable explanation for the origin of the selectivity of gold supported on iron oxide has been searched for, considering gold–iron interaction, metal particles size, and the nature of the different supports.

2. Experimental

2.1. Materials

Goethite (α-FeOOH), hematite (α-Fe_2O_3), alumina (γ-Al_2O_3), and iron-modified alumina were employed as supports.

Hematite and goethite were obtained by hydrothermal synthesis [12]. Goethite was prepared from a Fe(III) nitrate solution with a concentration of 0.53 M. NaOH, 2 M, was added to the solution in order to obtain a ferrihydrite precipitate. The solid was washed twice with bidistilled water and filtered. The ferrihydrite was aged in polyethylene vessels containing 0.3 M NaOH for 15 days at 60 °C. Finally, the sample was dried at 40 °C and calcined at 180 °C.

Hematite was obtained from Fe(III) nitrate solution and KOH at 90 °C. $NaHCO_3$ was added to this solution and the suspension was aged at this temperature at pH 8–9 in a polyethylene vessel for 2 days.

X-Ray diffraction patterns of the obtained goethite and hematite were obtained with a Siemens D5000 diffractometer using a Cu Kα radiation and 2 sets of 1° Soller slits and a graphite monochromator. The data were collected in the 2θ range: 15,800–140,000°, the scanning step was 0.025°, and 4969 points were measured with a counting time of 20 s per point.

Three samples of iron oxide supported on alumina were prepared. γ-Al_2O_3 (Rhone Poulenc, 77 m^2/g) was impregnated with solutions of $Fe(AcAc)_3$ (Aldrich, 99.99%) in toluene with concentration corresponding to a target iron load of the solid of 5, 10, and 20 wt%. Following 48 h of impregnation, the solid was filtered and washed with fresh solvent. The solids were calcined for 4 h at 450 °C. The three solids were named as 5FeAl, 10FeAl, and 20FeAl, where the number refers to the nominal iron load of the modified alumina.

Gold was fixed to hematite following the direct anionic exchange method, DAE [13]. A solution of $HAuCl_4$ (1×10^{-3}M) was added to the solid at 60 °C. The target gold concentration was of 1%. The suspension was stirred for 2 h at a constant pH of 4. Afterwards, a diluted ammonium solution was added in order to eliminate the chlorine species, which are considered to be responsible for gold particle growth during the following calcination steps [14]. The solid was filtered and washed several times with distilled water. Then, the sample was calcined at 300 °C for 3 h in chromatographic air. The sample was named as Au/HDAE. The same procedure was followed for preparing gold supported on 5FeAl, 10FeAl, and 20FeAl. These samples were named as Au/5FeAl, Au/10FeAl, and Au/20FeAl. In the case of goethite, a similar procedure was followed to prepare the corresponding catalyst (Au/G), but the calcination temperature was 120 °C to avoid the decomposition of this oxyhydroxide.

An additional catalyst, named as Au/HDP, was prepared using hematite as the support following the deposition–precipitation method.

The Au/Al_2O_3(Au/Al from now on) was kindly provided by Ivanova (from Dpto. de Química Inorgánica e Instituto de Ciencia de Materiales de Sevilla, Centro Mixto Universidad de Sevilla-CSIC, Avda. Américo Vespucio 49, 41092 Sevilla, Spain). The results corresponding to the preparation and characterization of this sample can be found in Ref. [14]

2.2. Characterization of the samples

The content of iron and gold in the catalysts was determined by ICP-AES.

The specific surface area of the supports was measured by BET method in a BET NOVA 1200e apparatus.

As the electric charge of the support surface is a crucial parameter for the DAE preparation method, the isoelectric points (IEPs) of the supports were determined. In pursuing these, potentiometric titrations were carried out. A KNO_3 solution (100 cm^3 and 0.1 M) was added to the solid (approximately 0.3 g). The pH of the suspension was set at 3 by addition of a solution of 0.1 M HNO_3. Afterward, 0.02-cm^3 aliquots of 0.1 M KOH solution were added to the suspension, and the pH was measured after 5 min of stabilization. The experiment was carried out at 1 atm of N_2 at 30 °C. A blank titration (the electrolyte solution) was also performed.

Gold particle size was studied by means of Transmission Electron Microscopy (TEM) in a JEOL 100CX2 (Tokio, Japan). Approximately 100 gold particles were measured to determine the particle size distribution. The average diameter of the crystals in the different catalysts was calculated from the following formula: $d = (\sum n_i d_i)/n_i$.

The reducibility of the supports and the catalysts was analyzed with temperature programmed reduction (TPR) in a homemade equipment. Before reduction, the samples were treated with flowing Ar at 300 °C (120 °C for goethite). Then, a flowing mixture (20 ml/min) of 10% H_2/Ar was introduced, raising the temperature at 8 °C/min from room temperature up to 550 °C. The TPR profile was obtained following the H_2 consumption with a TCD detector.

X-ray absorption measurements of Au/5FeAl were performed at D04B-XAS beam lines of the Laboratório Nacional de Luz Síncrotron (LNLS, Campinas, Brazil). The electron storage ring was operated at 1.37 GeV with a nominal current of 130 mA. XANES spectra were obtained in transmission and fluorescence modes at K-edge for Fe (7112 eV) and L_{III}-edge for Au (11919 eV) at room temperature, and at least three individual spectra were recorded and averaged. The data were collected at room temperature, and at least three individual spectra were recorded and averaged. Incident and transmitted X-ray fluxes were measured using an air-filled ionization chamber, and the beam was monochromatized with a "channel cut" Si(1 1 1) monochromator. XANES spectra at the Fe K-edge were collected in the range 6950–7350 eV. The energy step and counting time were 0.5–1 eV and 3 s; at the Au L_{III}-edge, the data were collected in the range 11,850–12,150 eV, with the same energy step and counting time mentioned above. The energy was calibrated at the inflexion point of edge jump in the XANES spectrum of the respective metallic foils. The spectra were background corrected using a linear fit in the region before the pre-edge and normalized close to the pre-edge border.

2.3. Catalytic test

The hydrogenation of crotonaldehyde and cinnamaldehyde was carried out in a 40-ml batch reactor at 100 °C and 1 MPa of H_2. Twenty milliliters of a solution of the corresponding aldehyde (0.08 M) in isopropanol and approximately 200 mg of catalyst were employed in each run. The stirring rate was 300 rpm. The selectivity to the different products (see Fig. 1) and the conversion of the unsaturated aldehyde were measured during 3 h of the reaction time.

For Au/HDAE, the stirring rate was varied in the range 300–900 rpm. Within this range the conversion/selectivity pattern of the catalyst was the same for the different stirring rates. Thus the lack of external diffusion limitations was confirmed.

The analysis of reactants and products was preformed in a chromatograph, provided with a FID detector and a Chrom PAW col-

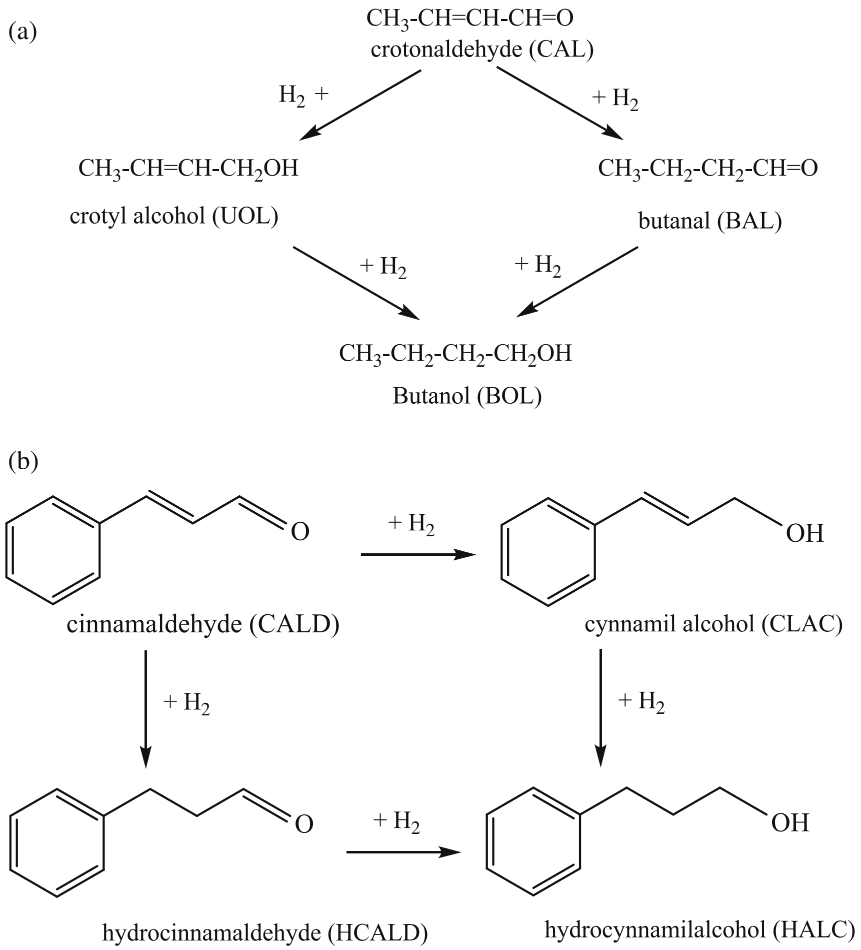

Fig. 1. Reactants and products in the hydrogenation of (a) crotonaldehyde, and (b) cinnamaldehyde.

umn, operating at 35 °C (hydrogenation of crotonaldehyde) or 70 °C (hydrogenation of cinnamaldehyde).

3. Results

3.1. Synthesis of the catalysts

The XRD analysis of the supports goethite and hematite corroborates that the solids obtained by hydrothermal synthesis corresponds αFeOOH and α-Fe_2O_3, respectively. For the FeAl samples (iron oxide supported on γ-Al_2O_3), the XRD pattern matches with the pattern corresponding to γ-Al_2O. No signal corresponding to iron oxides was detected probably due to the high dispersion achieved by iron species on alumina surface.

Following DAE method of preparation, the different supports were put in contact with solutions of $HAuCl_4$. Under the working pH conditions (pH = 4), the most stable gold species is the anionic complex $[AuCl_2(OH)_2]^-$ [12]. Since the IEP of the supports was in the 7–9 range (see Table 1), all the solid surfaces were positively charged at the experimental conditions. Thus, the gold anionic complex is attracted by the support surface and it becomes anchored to the solid by exchanging one or two OH groups of the oxide surface [14]. Hematite and goethite fix the whole of the metal in the precursor solution, which corresponds to a target loading of 1% of gold showing that both iron oxides have a relatively high concentration of OH that could be exchanged with the gold complex. In the case of bare alumina and FeAl, the concentration of $HAuCl_4$ in the preparation solution should be increased in order to obtain a similar gold loading as in the case of hematite and goethite. This fact shows that only a low fraction of OH of these supports is active for the anchoring of gold complexes in spite of their large specific surface area.

Table 1
Properties of the supports and the corresponding catalysts.

Sample	Surface area (m^2/g)	IEP	%Fe	%Au	TEM *d* (nm)	H_2/Fe
γ-Al_2O_3	77	7.2	0	0	–	–
α-FeOOH	27	9	0	0	–	0.21
α-Fe_2O_3	26	8.4	0	0	–	0.18
5FeAl	76	8.0	10	0	–	0.17
10FeAl	76	8.2				0.16
20FeAl	74					0.16
Au/Al	77	–	0	1.5	< 4	0
Au/G	27	–	98.8	1.4	12–15	0.22
Au/5FeAl	77	–	5	1.1	4.3	0.15
Au/10FeAl	74	–	10	1.0	–	0.15
u/20FeAl	–	–	20	1.0	5.3	0.16
Au/HDP	26	–	99	1.1	7.7	0.16
Au/HDAE	26	–	99	1.2	5.7	0.17

3.2. Characterization

XRD analysis of the catalysis showed that the crystal structure of the supports was not modified upon the introduction of gold.

The gold mean particle diameter corresponding to the different catalysts was measured by TEM, and is reported in Table 1.

The highest value of gold crystals was found for gold supported on goethite, with a mean particle diameter of 15 nm. In Fig. 2, some relatively large gold particles can be observed. In this image, a gold crystal of 9.1 nm is indicated with an arrow; one can clearly observe the spherical morphology of this particle, suggesting a low support–metal interaction.

For the Au/Al sample, the mean gold particle size could not be measured from TEM due to the low contrast between the support and the metal particles. Previously, XRD data of this sample indicated that gold crystals are lower than 4 nm [14].

The sample prepared on hematite by DAE presents a mean particle size of 6.7 nm. Some gold crystals supported on hematite can be observed in Fig. 3. The other catalyst obtained from hematite, Au/DP, shows a higher mean particle size (8.7 nm) than Au/HDAE.

The success of DAE method for preparing gold nanoclusters on iron oxide supports strongly depends on their nature, as could be expected. On goethite, small gold crystals cannot be achieved probably due to the high IEP of this oxyhydroxide. It was established that an oxide should posses an IEP close to 6–7 in order to obtain small gold crystals [13,15]. The IEP corresponding to hematite is lower than the one of goethite. In line with this, the size of the gold particle supported on hematite is notably smaller than that of the gold particle supported on goethite. The oxides obtained by supporting iron on γ-Al_2O_3 (FeAl series) present an IEP value between those corresponding to the parent oxides. Following this, gold crystal sizes obtained on FeAl are much lower than the ones on bare hematite or goethite.

The XANES spectra of Au/5FeAl (calcined at 300 °C) were measured in both Fe K- and Au L_{III}-edges. Fig. 4 shows the XANES result for this catalyst as well as for the compounds used as reference. The first Fe K prominent signal of the catalyst appears at 7133.5 eV, and the energy position coincides with that of the Fe^{3+} reference (α-Fe_2O_3), confirming that Fe is present in the catalyst in its trivalent state. At the Au L_{III} border, the first signal of the analyzed sample appears at 11923 eV, in this case coincident with the Au^0 profile, showing that gold supported on FeAl is in metallic state.

Hutchings et al. carried out an extensive characterization of Au/Fe_2O_3 with a set of different techniques (XANES being one of them) [16]. These authors concluded the presence of cationic gold on a 5%Au/Fe_2O_3 sample. Other studies have also determined the presence of cationic gold on similar catalysts [17]. Thus, our results obtained from XANES spectra are not in agreement with the previous studies. Since the thermal history of the samples has a profound influence on the properties of gold supported on iron oxide [16], the different calcination pretreatments performed over the sample would account for these differences.

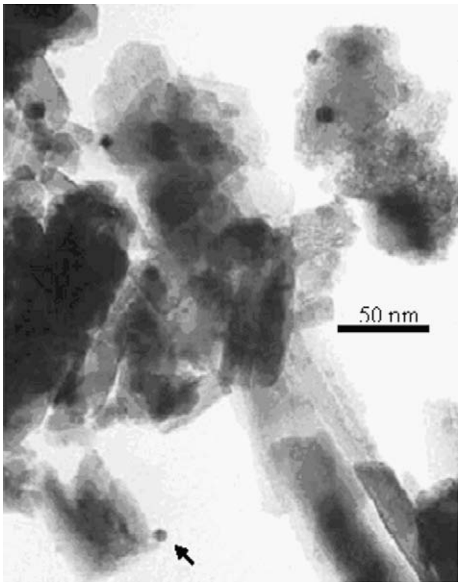

Fig. 2. TEM image corresponding to Au/GDAE sample.

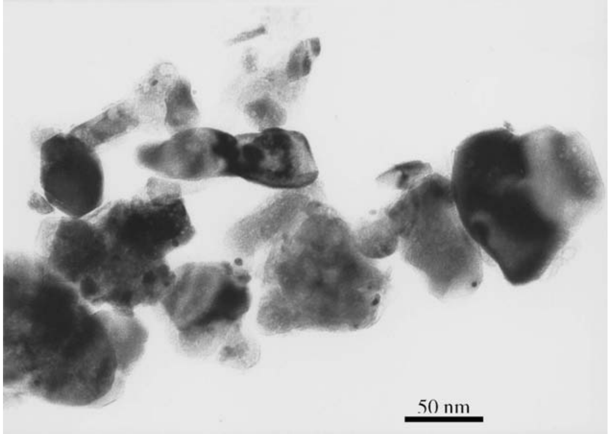

Fig. 3. TEM image corresponding to Au/HDAE sample.

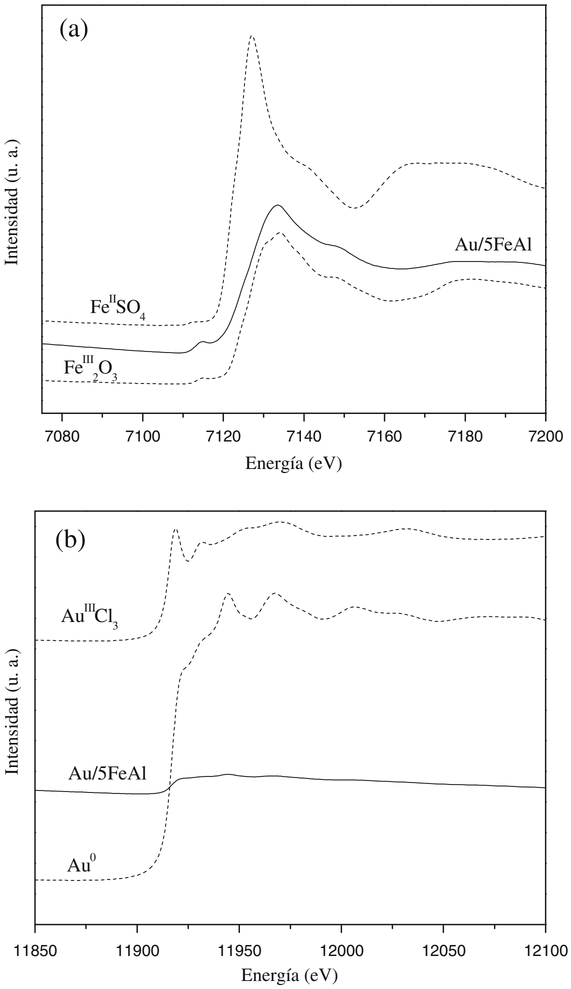

Fig. 4. XANES at the (a) Fe K-, and (c) Au L_{III}-edges for sample Au/5FeAl. Spectra of reference compounds are also presented.

TPR measurements were carried out over the supports and the gold catalysts in order to investigate the changes of reducibility introduced by the noble metal.

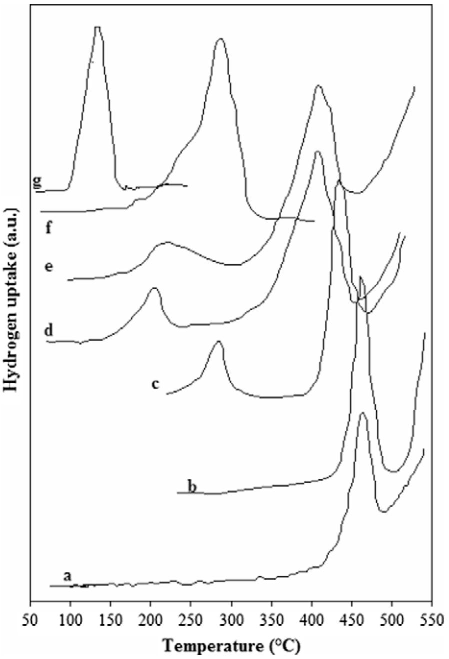

Fig. 5. TPR profiles of supports and gold catalysts. (a) α-Fe_2O_3; (b) α-FEOOH; (c) Au/G, (d) Au/HDAE, (e) Au/HDP, (f) Fe5Al, and (g) Au/Fe5Al.

For the bare supports, hematite, and goethite (Fig. 5, profiles a and b, respectively), similar trends were observed due to the fact that goethite undergoes a transformation toward hematite during TPR measurements. For both cases, a sharp peak centered at approximately 450 °C is observed. A second consumption (not completely observed for the present experimental conditions) was also detected. The specific hydrogen consumption corresponding to the first peak is reported in Table 1 as mole of H_2 per mole of iron. It can be calculated that the first consumption accounts for the reduction of Fe_2O_3 to Fe_3O_4 (magnetite). The second consumption is related to the reduction of magnetite to FeO.

The TPR measurement of 5FeAl is shown in Fig. 5, profile f. A peak at 280 °C with a shoulder at a lower temperature is observed. The reduction of iron species occurs at a much lower temperature than the one corresponding to hematite, showing that supporting iron oxides on alumina decreases the reducibility. However, the specific amount of H_2 consumed by this sample (see Table 1) is similar to the one corresponding to hematite. The other two systems, 10FeAl and 20FeAl, show similar trends as 5FeAl (not shown in Fig. 5, for the sake of simplicity).

Upon the introduction of gold to the supports hematite and goethite, the corresponding TPR profiles are modified. The peak formerly observed at approximately 450 °C for hematite and goethite is shifted to lower temperatures. Besides, a broad consumption at temperatures lower than 300 °C is observed for both Au/HDP and Au/HDAE. In the case of goethite, a peak at 400 °C is observed. The amount of hydrogen corresponding to the peaks observed in TPR accounts for the reduction of hematite to magnetite. Hence, it could be argued that gold species are not engaged in the reduction processes detected by TPR.

For Au/5FeAl, the consumption peak is shifted 100 °C to a lower temperature than that corresponding to gold-free sample. The reduction of iron species starts at notably low temperature: approximately 100 °C. Gold species are not responsible for this low reduction process in the Au/5FeAl sample since no cationic gold is present, following XANES results. In spite of the high reducibility of iron supported on alumina, the specific amount of H_2 engaged in the reduction is similar to the one observed for hematite.

The TRP results of Au/10FeAl and Au/20FeAl show similar trends to those observed in Au/5FeAl.

Goethite, hematite, and iron supported onto alumina should be considered as reducible oxides since iron species undergo reduction at temperatures lower than 450 °C, following TPR results. Their reducibility is enhanced by the presence of gold nanoparticles. A diminution of the reduction temperature of the support due to the presence of the noble metal was also observed for gold supported on different oxides: ceria [18], hematite [4,19,20], and goethite [19]. Dissociation of hydrogen occurs on gold surface [17,21], and would be the origin of this increased reducibility.

Besides, an effect of gold particle size on the reducibility of the support was observed. The smaller the particle size, the higher the effect on the reducibility of iron species. To label, the smallest gold crystals are observed on γ-Al_2O_3 modified with 5% of iron (5FeAl) for which the reduction starts at the lowest temperature (100 °C). On the other hand, goethite possessing the highest particle size starts reduction at the highest temperature among all the samples. These results are in agreement with the fact that the amount of corner, edges, defects on gold surface increases with decreasing particle size in the range of 1–10 nm [22]. Hence, it could be concluded that the availability of reducing hydrogen species is the highest for Au/5FeAl with the lowest particle size.

3.3. Hydrogenation of crotonaldehyde and cinnamaldehyde

Firstly, experiments were carried out employing the catalyst and the reactive mixture in the absence of the reductant. No appreciable conversion of the substrates was observed, showing that no hydrogen transfer from the solvent (isopropanol) to the aldehyde could occur.

The reaction progress of the hydrogenation of crotonaldehyde over for Au/Al, Au/HDAE, Au/G, and Au/10 FeAl catalysts is shown in Fig. 6. Similar results are reported in Fig. 7 for the hydrogenation of cinnamaldehyde. The reaction progress corresponding to Au/G is not reported in Fig. 7 since too low conversion levels were attained for reaction time lower than 3 h.

In Table 2, the specific activity of all the prepared catalysts attained at 3 h of the reaction is reported as moles of aldehyde (crotonaldehyde or cinnamaldehyde) converted per second and per gram of gold for all the studied catalysts. The selectivities to the desired products, crotyl and cinnamyl alcohols, are also reported in Table 2 for the same reaction time.

During the hydrogenation of crotonaldehyde no other products than the hydrogenation ones (shown in Fig. 1a) were detected. On the contrary in the case of cinnamaldehyde, styrene was observed, showing that a decarbonylation of this aldehyde occurs. Trying to

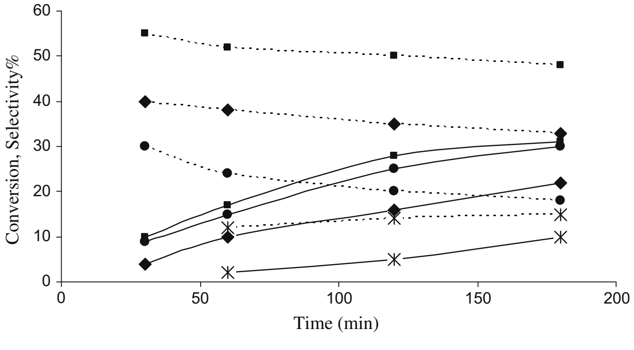

Fig. 6. Conversion of crotonaldehyde (—) and selectivity to crotyl alcohol (---) for: Au/Al (●), Au/Fe10Al (◆), Au/G (*), and Au/HDAE (■).

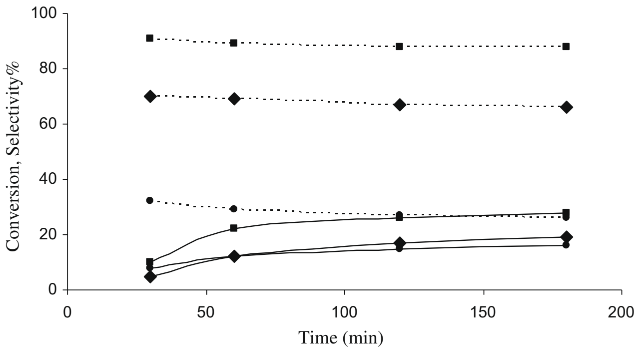

Fig. 7. Conversion of cinnamaldehyde (—) and selectivity to cinnamyl alcohol (---) for: Au/Al (●), Au/Fe10Al (◆), and Au/HDAE (■).

focus on the efficiency of the catalyst to selectively hydrogenate the C=O bond against the C=C bond, this product was not taken into account for calculating the selectivity reported in Table 2 and in Fig. 7.

The conversion of crotonaldehyde attained at 3 h of the reaction time by Au/Al was 30%, while the selectivity to crotyl alcohol was 18%. In Fig. 6, it can be observed that selectivity to the desired product decreases with time. The diminution of the selectivity is due to an increase of the production of butanol.

In the case of the hydrogenation of cinnamaldehyde, the selectivity to the unsaturated alcohol was higher at any time than for the case of the hydrogenation of crotonaldehyde. The steric protection of the double bond in the case of cinnamaldehyde would account for this difference.

In Au/Al, gold nanoparticles are supported on an inert carrier. Thus, the selectivity values would arise from the intrinsic catalytic properties of gold, free from any effect of the support under the present reaction conditions.

The conversion levels measured over Au/HDAE are higher than those corresponding to Au/Al (see Figs. 6 and 7). The same trends were observed for the Au/HDP sample (results not shown in Figs. 6 and 7 for the sake of simplicity). Furthermore, the activities (expressed as mole of aldehyde converted per gram of gold and per second) attained for the catalysts supported on α-Fe_2O_3, Au/HDP and Au/HDAE, are slightly higher than that of the alumina-supported sample. This is an interesting result considering that gold particle size corresponding to hematite-supported catalysts are higher than the one of Au/Al. Thus, it could be concluded that iron oxide increases the intrinsic activity of gold.

The selectivity to crotyl alcohol measured over gold supported on α-Fe_2O_3 is sensibly higher than for Au/Al, as can be observed in Fig. 6. The same trend is observed for the hydrogenation of cinnamaldehyde (see Fig. 7 and Table 2). The higher performance achieved by the hematite-supported samples against alumina-supported one would be due to a promoter effect of the iron oxide on gold, increasing the rate of the hydrogenation of C=O against C=C. It is difficult to exactly describe the nature of the promotional effect of iron. The possibility of an electronic transfer from the support to metal particles [3,4] is unlikely for our reaction conditions. The formation of Fe^{2+} species (that would be responsible for such an electronic transfer) would not occur since the reaction temperature is 100 °C and hematite starts reduction at approximately 200 °C, following TPR results. We will revert to this matter later.

When comparison is made between the two catalysts prepared on α-Fe_2O_3, Au/HDAE, and Au/HDP, only slight differences are detected: the selectivities toward crotyl alcohol and toward cinnamyl alcohol as well as the activities are approximately the same for both samples. Keeping in mind that gold mean particle size of Au/HDP is different from the one of Au/DAE, it could be concluded that no influence of this parameter exists on the catalytic properties of gold supported on hematite. In this sense, these samples present a different behavior than Au/Al_2O_3 catalysts studied by Bus et al., for which a size dependence of selectivity was observed [11]. The origin of this phenomenon was ascribed by the authors to a stronger dependence of the C=O hydrogenation rate on cluster size compared to C=C hydrogenation rate, but the sizes of the gold particles (1 nm) were much more small than those of the ones supported on hematite (7.7, 5.7 nm).

The Au/G catalyst showed the lowest conversion among the studied samples, namely 10% at 3 h. The meager reactivity of Au/G is probably related to the high gold particle size of this sample (15 nm from TEM results). If hydrogen species are located at Au atoms at corner and edge positions and if no spill over of hydrogen onto Au atoms at the faces occurs [23], a low reactivity of gold particles supported on goethite should be expected. Moreover, if we assume a cuboctahedral shape for gold crystals, it can be considered that for a particle size of 13 nm the fraction of Au atoms at corner and edges is extremely low (lower than 0.08 according to Pradier et al. [24]).

For Au/G, the selectivities toward crotyl alcohol and toward cinnamaldehyde were 15% and 23%, respectively, which were measured at 3 h of the reaction time. Both values are not higher than the one corresponding to the sample supported on inert alumina. In order to compare selectivities at the same level of conversion, in an additional experiment the hydrogenation of crotonaldehyde was carried out for 6 h (instead of 3 h). For this reaction time, the conversion was 29% and the selectivity toward crotyl alcohol was quite similar to that shown by Au/Al, showing that the promotional effect of the iron is not present when goethite is the support. Probably the high particle size as well as the low interaction between the support and the gold crystals is the origin of the low performance of Au/G for the selective hydrogenation of α,β-unsaturated compounds.

Table 2
Catalytic properties of gold-supported catalysts for the hydrogenation of crotonaldehyde and cinnamaldehyde measured at 3 h of the reaction time.

Catalyst	Act. croton. (10^5)[a]	X croton. (%)	S (%) crotyl	Act. cynnamald.	X (%)[b]	S (%) cinnamyl
Au/Al	1.9	30	18	0.9	16	26
Au/G	0.6	10	15	0.3	4	23
	1.6[b]	25[b]	20[b]	–	–	–
Au/5FeAl	1.8	21	35	1.5	20	67
Au/10FeAl	2.0	22	33	1.6	19	66
Au/20FeAl	1.8	20	38	1.0	12	–
Au/HDP	2.1	28	45	2.0	26	86
Au/HDAE	2.4	31	48	2.0	28	88
Pt/Al_2O_3	10.8	100	2	8.1	100	5

[a] Moles converted per second and per gram of gold following 3 h of reaction.
[b] Measurement at 6 h of reaction.

The activity for the hydrogenation of crotonaldehyde and the selectivity to the unsaturated alcohol corresponding to the Au/FeAl series are higher than the ones of Au/Al (see Table 2). Once again a beneficial effect of iron species on gold is observed. It is worth noting that only metallic gold would be present in Au/5FeAl catalyst, following XANES result and that Au^0 should be responsible for the activity and high selectivity of this sample. In this sense, the nature of the active site for the hydrogenation of C=O bond over Au/Fe_2O_3 is completely different from that corresponding to CO oxidation at low temperature, for which the high activity is predicated on the presence of cationic gold [17,25]. In a previous work by some of us, regarding the hydrogenation of crotonaldehyde over an Au/CeO_2 catalyst [6], XPS measurements indicated that only metallic gold was present in the highly selective catalyst.

It is interesting to observe that Au/20FeAl shows particle size similar to that shown by Au/HDAE. In spite of this similarity, the selectivities are quite different for each case. Besides, the reducibility of Au/FeAl is higher than that of Au/H, following TPR results. Fe^{2+} species could be present in Au/FeAl under reaction conditions since it was established that iron supported on alumina starts reduction at 100 °C (see Fig. 5). Thus, the higher selectivity of the samples supported on hematite against those on FeAl could not be linked to redox properties of the support, at least in a straightforward way.

Taking into account the consideration commented above, the nature of the promotional effect of iron species on the intrinsic selectivity of gold is unclear. However, some aspects could be concluded: (i) the reducibility of iron species is not linked with the beneficial effect of iron on gold, (ii) gold particle size has no substantial effect on the activity/selectivity of gold supported on iron oxide, and (iii) iron species are not responsible for the stabilization of other gold species than metallic ones.

More likely we suggest that the nature of the different iron oxides, α-Fe_2O_3 and iron supported on γ-Al_2O_3, influences the morphology of gold particles, giving rise to a particular particle shape in which the sites related with the increase of C=O hydrogenation against C=C hydrogenation prevail. The hydrogenation of α,β-unsaturated compounds would be structure-dependent as has been suggested for the oxidation of CO over $Au/Mg(OH)_2$ [26], and the hydrogenation of acrolein over Au/TiO_2 and Au/ZrO_2[10]. Many sites have been proposed as selective for the activation of C=O group, for example the close packed structure of the (1 1 1) plane [27,28] and interfacial sites [8,29]. Certainly, we could not determine unambiguously the relative concentration of the different sites on gold surface in the light of the results of the present work. However, we suggest that iron oxides, mainly hematite, promote the formation of a selective morphology of gold crystals.

4. Conclusions

- Gold nanostructures supported on iron oxides are more selective than gold supported on an inert oxide in the hydrogenation of crotonaldehyde and cinnamaldehyde.
- The high selectivity of gold supported on iron oxides would not be related to redox properties of the support.
- Gold particle size does not have great influence on the selectivity toward the hydrogenation of C=O.
- The morphology of gold particles influences the selectivity in the hydrogenation of α,β-unsaturated compounds.

References

[1] P. Claus, A. Brucker, C. Mohr, H. Hofmeister, J. Am. Chem. Soc. 122 (2000) 11430.
[2] J.E. Bailie, H.C.A. Abdullah, J.A. Anderson, C.H. Rochester, N.V. Richardson, N. Hodge, J.G. Zhang, A. Burrows, C.J. Kiely, G.J. Hutchings, Phys. Chem. Chem. Phys. 3 (2001) 4113.
[3] C. Milone, R. Ingoglia, A. Pistone, G. Neri, F. Frusteri, S. Galvagno, J. Catal. 222 (2004) 348.
[4] C. Milone, R. Ingoglia, L. Schipilliti, C. Crisafulli, G. Neri, S. Galvagno, J. Catal. 236 (2005) 80–90.
[5] R. Zannella, C. Louis, S. Giorgio, R. Touroude, J. Catal. 223 (2004) 328.
[6] B. Campo, S. Ivanova, M. Volpe, R. Touroude, J. Catal. 242 (2006) 162–171.
[7] B. Campo, C. Petit, M. Volpe, J. Catal. 254 (2008) 71.
[8] J. Baile, G. Hutchings, Chem. Commun. (1999) 2151.
[9] S. Schimpf, M. Lucas, C. Mohr, U. Rodemerck, A. Bruckner, J. Radnik, H. Hofmeister, P. Claus, Catal. Today 72 (2002) 63.
[10] C. Mohr, H. Hofmeister, P. Claus, J. Catal. 213 (2003) 86.
[11] E. Bus, R. Prins, J.A. van Bokhoven, Catal. Commun. 8 (2007) 1397.
[12] U. Schwertmann, R. Cornell, Iron Oxides in the Laboratory: Preparation and Characterization, Wiley-VCH, 2000. p. 188.
[13] S. Ivanova, C. Petit, V. Pitchon, Appl. Catal. A 267 (2004) 191.
[14] V. Pitchon, Y. Zimmermann, C. Petit, Appl. Catal. A. Gen. 298 (2006) 57.
[15] R. Zanella, S. Giorgio, C.R. Henry, C. Louis, Phys. Chem. 106 (2002) 7634.
[16] G. Hutchings, M. Hall, A. Carley, P. Landon, B. Solsona, C. Kiely, A. Herzing, M. Makkee, J. Moulijn, A. Overweg, J. Fierro-Gonzalez, J. Guzman, B. Gates, J. Catal. 242 (2006) 71.
[17] F. Boccuzzi, A. Chiorino, M. Manzoli, D. Andreeva, T. Tabakova, J. Catal. 188 (1999) 76.
[18] S. Ivanova, V. Pitchon, C. Petit, J. Mol. Catal. A 256 (2006) 278.
[19] B. Campo, O. Rosseler, M. Alvarez, E. Rueda, M. Volpe, Mater. Chem. Phys. 109 (2008) 48.
[20] L.I. Ilieva, D. Andreeva, A. Andreev, Thermochim. Acta 46 (1997) 169.
[21] D. Barton, S. Podkolzin, J. Phys. Chem. B 109 (2004) 2262.
[22] R. van Hardefeld, F. Hartog, Surf. Sci. 15 (2) (1969) 189.
[23] E. Bus, J. Miller, J. van Bokhoven, J. Phys. Chem. B 109 (2005) 14581.
[24] C.M. Pradier, T. Brichem, Y. Berthier, G. Cordier, Catal. Lett. 29 (1994) 371.
[25] R.M. Finch, N.A. Hodge, G.J. Hutchings, A. Meagher, Q.A. Pankhurst, M.R.H. Siddiqui, F.E. Wagner, R. Whyman, Phys. Chem. Chem. Phys. 1 (1999) 485.
[26] D. Cunningham, W. Vogel, H. Kageyama, S. Tsubota, M. Haruta, J. Catal. 177 (1998) 1.
[27] M. Englishch, V. Ranade, J. Lercher, Appl. Catal. A 161 (1997) 111.
[28] P. Claus, H. Hofmeister, J. Phys. Chem. B 103 (1999) 2766.
[29] C. Mohr, H. Hofmeister, J. Radnik, P. Claus, J. Am. Chem. Soc. 125 (2003) 1905.